Flux Pinning and Intergranular Critical Current Density Study in $SmBa_2Cu_{3-x}Fe_xO_7$ Superconductor

M.I. Youssif [1,2] and A. Sedky [3,4]

[1]Physics Department, Faculty of Science at New Damietta, Damietta University, New Damietta 34517, Egypt
[2] Physics and Astronomy Department, Collage of Science, King Saud University, P.O. Box 2455, Riyadh 11451, Saudi Arabia
[3]Physics Department, Faculty of Science, Assiut University, Assiut, Egypt
[4] Physics Department, Faculty of Science, King Faisal University, Al-Hassa 31982, Saudi Arabia
sedky1960@yahoo.com; youssifm@yahoo.com

Abstract: Low field ac magnetic susceptibility study for $SmBa_2Cu_{3-x}Fe_xO_7$ superconductors with various x values ($0.00 \le x \le 0.06$) is reported. The results of ac susceptibility are used to determine the pinning force density and intergranular critical current density. However, two different values of q factor obeying the law $(1 - \frac{T_m}{T_c}) = a_L (H_m)^q$ are extracted from the slope of each plot. The first corresponds to smaller field ($0.00 \le H_m \le 300$ A/m), and its values are between 0.19 and 0.66. While, the second corresponds to higher field (300 A/m $\le H_m \le$ 600 A/m) and its values are between 0.30 and 0.91. Compared to pure sample, the pinning force density is decreased by 0.01 of Fe addition, followed by an increase with further increase of Fe up to 0.06. Similar behavior is obtained for intergranular critical current density. These results are discussed in terms of induced weak link which is produced by Fe doping in Sm: 123 superconductors.

[M.I. Youssif and A. Sedky, **Flux Pinning and Intergranular Critical Current Density Study in $SmBa_2Cu_{3-x}Fe_xO_7$ Superconductor.** *J Am Sci* 2015;11(7):42-48]. (ISSN: 1545-1003). http://www.jofamericanscience.org. 6

Keywords: Ac susceptibility; SmBCO; Critical current; Weak- link

1. Introduction

Since the discovery of Y: 123 superconductors, lot of work have been done to improve its critical current density J_c for considered applications such as power cables and magnetic levitation. [1-3]. It is generally accepted that strong defect pinning centers for flux lines in superconductors are required for J_c enhancement. The flux pinning densities in these materials helps for understanding their transport and magnetic properties. AC magnetic susceptibility measurements proved to be one of the most powerful methods toward this goal [4-8]. Early, ac susceptibility measurements are analyzed in terms of Müller model for estimating the pinning force densities in the matrix through weak links [9]. In addition, several models are employed to analyze the temperature and ac field variation of ac susceptibility. In terms of these models, the temperature and field variations of the critical current density J_c are estimated [10-23].

The effect of partial substitution for Cu sites with 3d elements on the transport and magnetic properties of Y: 123 systems have been extensively investigated. Great attention is focused on Fe doping owing to the co-existence of magnetic ordering by Fe sublattice and superconductivity [24-26]. It is found that Fe atom attracts additional oxygen atoms, and consequently the Fe coordination number will be increased. A slight change of superconducting transition temperature T_c is observed for the samples of lower Fe content (≤ 0.05). But the further increase of Fe content leads to the abrupt decreasing of T_c, and the structure from orthorhombic to tetragonal phase occurs. On the other hand, two different types of irreversibility line behavior $(1 - \frac{T_m}{T_c}) \approx a(H)^q$ of $T_m(H)$, obeying law, have been found. The first corresponds to the pure Y: 123, and the other corresponds to Fe doped samples. These results indicate that the intergranular pinning force densities are decreased by Fe doping due to creation of an induced weak-link network inside superconducting grains [6, 25, 27, 28].

From the above background, it is obvious that the question of Fe placement in Cu sublattice of R: 123 superconducting systems is not completely clear. Therefore, we presented here the results of low field AC susceptibility measurements of $SmBa_2Cu_{3-x}Fe_xO_7$ samples with various x values ($0.00 \le x \le 0.06$). This study is focused on low ac fields below the first Abrikosov field for studying the effects of Fe doping on irreversibility line, flux pinning density and critical current density of Sm: 123 superconductors.

2. Experimental Details

$SmBa_2Cu_{3-x}Fe_xO_7$ samples with x = 0.00, 0.01, 0.03 and 0.06 are prepared by the well known solid state reaction method. The ingredients of Sm_2O_3, $BaCo_3$, CuO and Fe_2O_3 of 4 N purity are thoroughly

mixed in the required proportions and then calcined at 910°C in air for a period of 24 h. This exercise is repeated three times with intermediate grinding at each stage. The resulting powders are ground, mixed, palletized and annealed in flowing oxygen at 960 °C for a period of 24 hours and then the furnace cooled to room temperature with an intervening annealing for 24 hours at 600 °C. The samples are then characterized for phase purity by X-ray powder diffraction with Cu Kα radiation. The real (χ') and imaginary (χ") components of AC susceptibility are measured using AC susceptometer based on the mutual inductance method. The samples are placed in the holder and the field is applied parallel to the longest dimension of the samples. The measurements are made at 1012 Hz in the temperature range of (77-100 K), and at different values of ac field amplitudes H_m (26-600 A/m).

3.Results and Discussion

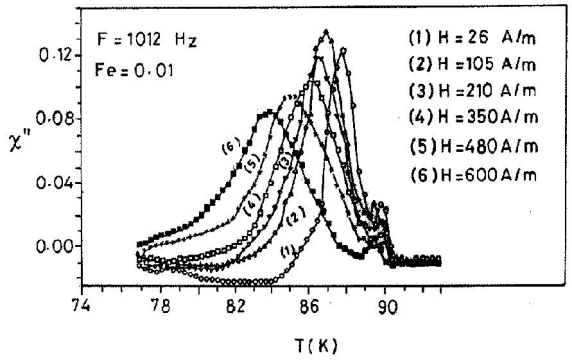

Figure 1 (a): χ" versus temperature at different values H_m for Fe = 0.01 sample

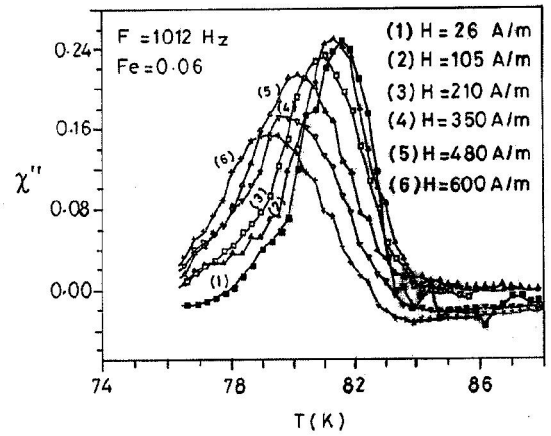

Figure 1 (b): χ" versus temperature at different values H_m for Fe = 0.06 sample.

The thickness of the samples is found to be 3.13, 5.3, 3.9 and 2.81 mm, respectively. The XRD patterns of samples indicate that the samples with x = 0.00, 0.01 and 0.03 are clearly orthorhombic single phase, while the sample with x = 0.06 is tetragonal. The lattice parameters and orthorhombic distortion for all samples are listed in Table 1. It clear that orthormbic distortion OD is gradually decreased from 0.018 to 0.00 by increasing Fe up to 0.06, which is consistent with the previous results which means that Fe doping effect only Cu-O chains, while the coupling between CuO_2 planes are unaffected.

Figure 1(a-b) shows the imaginary component of ac susceptibility χ" versus temperature and at different values of ac field amplitude H_m. The values of diamagnetic transition $T_c(\chi')$ listed in Table 1 are 90.3, 90, 88.5 and 83 K, for all samples. However, two different peaks in the imaginary part of ac susceptibility are clearly seen in Fig. 1. The first peak occurs at high temperature and it is associated with the grains matrix transition T_g. While the other exists at low temperature T_m and is associated with the behavior of weak-link at the grain boundaries. Although, the values of $T_c(\chi')$ are nearly unchanged with increasing ac field amplitude for all samples, the values of χ' are shifted to lower values. The corresponding values of $T_c(\chi')$, T_m, $\chi'(T_m)$ and $\chi''(T_m)$, χ' ($T < T_m$) and χ' ($T > T_m$) are listed in Tables (3-6). Figure 2(a) shows the variation of T_m against Fe content and at different values of ac field amplitude. It is found that T_m is increased by Fe followed by a decrease with further increase of Fe up to 0.06. On the other hand, the dependence of T_m on ac field amplitudes and at different values of Fe is presented in Figure 2(b). The common feature for all curves is the gradual decrease of T_m with increasing H_m. Two strongly distinct slopes are distinguished from the (T_m-H_m) curves. However, it has been reported that the value of $[dT_m/dH_m]$ is due to pinning centers force density of Josephson vortices [9, 25]. When $[dT_m/dH_m]$ is small, a strong pinning center occurs and the vise is versa at higher values of $[dT_m/dH_m]$. Two regions of different pinning center could be seen across the field region of the investigated samples. The first is occurs at ($0.00 \leq H_m \leq 300$ A/m), while the second occurs at ($300 \leq H_m \leq 600$ A/m). However, the behavior of $[dT_m/dH_m]$ against Fe content across the two regions is shown in Figure 2(c). It is observed that pinning force density increases with increasing Fe content in the low field region, as compared to pure sample. The behavior of pinning force density is not completely systematic, it is fluctuates around Fe content. On contrary, in the high field region, the pinning force density is decreased by 0.01 Fe, followed by an increase with further increase of Fe up to 0.06. Such behavior is presumably due to creation of induced new weak link structure inside superconducting grains by Fe doping [6, 25, 27].

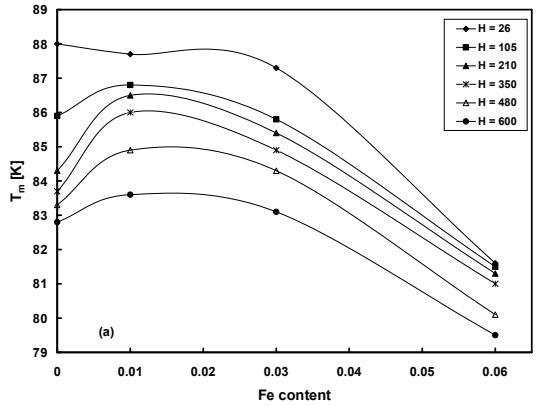

Figure 2 (a): T_m versus Fe content at different values of ac field amplitudes

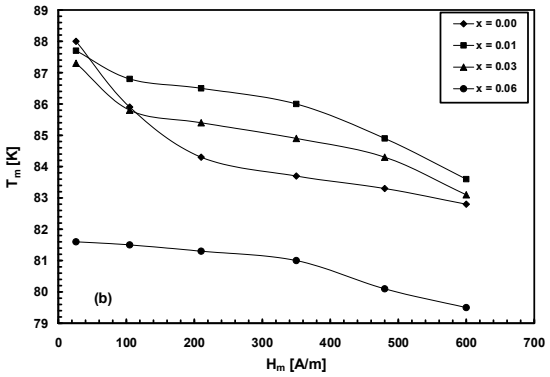

Figure 2 (b): T_m versus H_m at different values of Fe contents

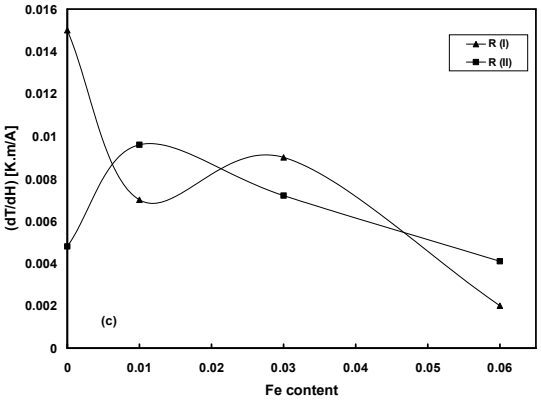

Figure 2 (c): Pinning force density versus Fe contents

The pinning force density displays non-monotonous character depending on Fe content. This is in agreement with the non monotonic behavior of screening capability of 0.12 Fe additions to Y: 123 under low dc fields [29].

According to Müller model, the AC low field dependence of irreversibility temperature ($T_{irr} \sim T_m$) is governed by the following equations [6,9];

$$(1+\frac{H_m}{H_j})^2 = 1+\frac{2\alpha_j(T)d}{\mu_0\mu_{eff}(T)H_j^2} \quad (1)$$

$$\mu_{eff}(T) = f_n + \frac{2f_s I_1 \lambda_g}{R_g I_0} \quad (2)$$

Here, f_n and f_s are the normal and superconducting volume fractions, λ_g is London penetration depth, R_g is the grain size, d is the sample thickness, $\mu_{eff}(T)$ is the effective permeability of Josephson medium, $\alpha_j(T)$ is the pinning force density, H_j is the characteristic field of critical state model, I_o and I_1 are the modified Bessel function of the first kind. Eq. (2) is valid for the fields larger than the lower Josephon field H_j when vortices nucleate along the grain boundary. These vortices are embedded in a diamagnetic medium of effective permeability μ_{eff} (T), and the temperature dependence is related to the London penetration depth as follows;

$$\lambda_g(T) = \lambda_g(0)[1-(\frac{T}{T_c})^4]^{\frac{-1}{2}} \quad (3)$$

For small fields used in the present investigation, we follow Müller model for flux creep dominated law for calculating the induced effect of pinning force density by as follows [6,9];

$$(1-\frac{T_m}{T_c}) = a_L(H_m)^q \quad (4)$$

where a_L is a parameter for the pure sample. The pinning force density $\alpha_j^p(0)$ is given by the following formula [6,9];

$$\alpha_j^p(0) = \frac{\mu_0 H_j}{d(a_L)^{\frac{1}{q}}} \quad (5)$$

But at higher applied field, the effective grain size starts to prevail over the London depth, resulting IL behavior. Then, Eq. (5) becomes;

$$\alpha_j^p(0) = \frac{\mu_0 H_j \lambda_g(0)}{dR_g(a_h)^{\frac{1}{q}}} \quad (6)$$

In contrast, for a small field, the field penetrates the grains with larger size, i.e. the grains are unaffected by Fe doping. As in the case of the pure sample, flux creep dominates over this region, and the IL obeys Eq.

5. By increasing AC field above 300 A/m, the field starts to penetrate the smaller size grains (Rg is lower for doped samples). Therefore, the IL crossover is observed at higher fields for Fe doped samples and the pinning force density is given by [6];

$$\alpha_j^p(0) = \frac{\mu_0 H_j}{2d(a_L)^{\frac{1}{q}}} \quad (7)$$

For simplicity we assumed that, the values of H_p at the peak are very close to AC field amplitudes H_m. The logarithmic plot between $\{1-(T_m/T_c)\}$ and H_m for pure and Fe doped samples is shown in Figure 3(a). One step crossover is observed in the slope of each plot. The crossover occurs as a result of the London penetration depth and the grain size variations. The values of (a) and (q) deduced from the fitting are listed in Table 2. In view of the above equations, the pinning force density is calculated in the two regions, and is shown in Figure 3(b). It is clear that $\alpha_j(0)$ is decreased by 0.01 Fe, followed by an increase with further increase of Fe up to 0.06. The values of $\alpha_j(0)$ are between 740 to 2163 (TA/m^2) for all samples. For pure sample, $\alpha_j(0)$ =1178 (TA/m^2) at small fields, and 1198 (TA/m^2) for 0.06 Fe doped sample. On the other hand, at high fields, $\alpha_j(0)$ is found to be 1918 (TA/m^2) and 2163 (TA/m^2) for pure and 0.06 Fe doped samples, respectively. Anyhow, these data are in good agreement with the reported data [5, 6, 9, 24].

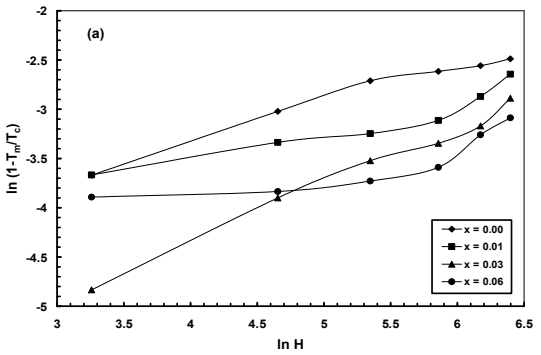

Figure 3 (a): Ln $\{1-(T_m/T_c)\}$ against H_m for pure and Fe doped samples

On the other hand, the values of AC susceptibility (χ' and χ'') are matched well with the reported data for a parallel-piped shape [10, 11, 13, 14, 18]. Therefore, the following equations are more suitable for J_c determination in the present case. The spatially averaged intergranular critical current density $J_c(T_m)$ at the peak temperature, T_m, is given by;

Where d is the sample thickness and H_p is the field at which the super current penetrates to the center of superconducting samples. Hence, we can also follow Refs. [11, 13, 18, 30] for the J_c determination over a wide range of temperatures as follows;

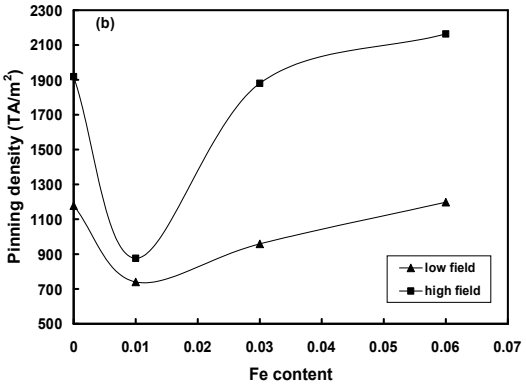

Figure 3 (b): Variation of pinning force density against Fe contents

$$J_c(T_m) = \frac{2H_P(T_m)}{d} \quad (8)$$

$$\chi'(T) = -\frac{0.5J_c(T)}{J_c(T_m)}, (T \succ T_m) \quad (9a)$$

$$\chi'(T) = -1 + \frac{J_c(T_m)}{J_c(T)}\left(1 - \frac{0.5J_c(T_m)}{J_c(T_m)}\right), (T \prec T_m) \quad (9b)$$

Therefore, $J_c(T)$ is easily calculated over a wide range of temperatures in terms of the values of $\chi'(T)$ and $J_c(T_m)$. In the present case, $J_c(T)$ is calculated at two different temperature regions, the first region lies between T_c and T_m, and the second region lies between T_m and 77 K. Figure 4(a-c) shows the variation of J_c against Fe contents at different values of H_m, and over a wide range of temperatures. These values are also listed in Tables (3-6).

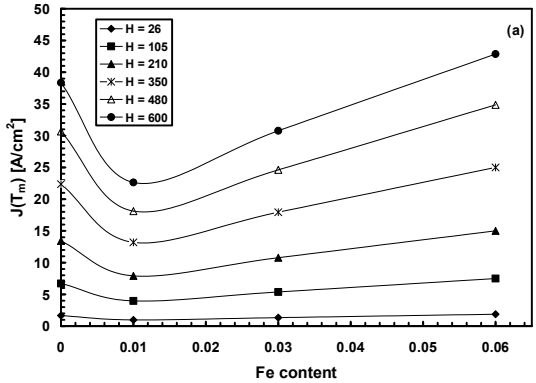

Figure 4(a): Critical current density J_c ($T = T_m$) against Fe contents at different values of ac field amplitudes H_m

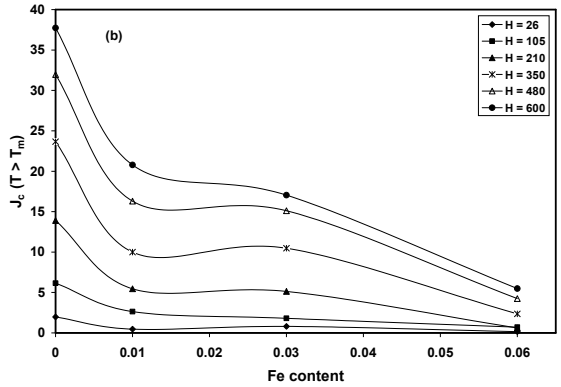

Figure 4(b): Critical current density J_c (T > Tm) against Fe content at different values of ac field amplitudes H_m

It is clear that the values of J_c are generally increased with increasing H_m, in agreement with the reported data [10, 11, 13, 14, 18, 30, 31]. But the values of J_c at T > T_m and at T < T_m are generally decreased by Fe up to 0.06, while the values of J_c at T =T_m are decreased at 0.01 Fe addition, followed by an increase up to 0.06 Fe. Furthermore, the values of J_c for 0.06 Fe sample is higher than that of sample.

Based on the above results, we can attribute the increase of pinning force density and intergranular current density with the addition of Fe to the improvement in the induced weal-link produced by Fe doping. This could be related to either some change in the grain size or decreasing the distance between the adjacent superconducting grains [9, 31].

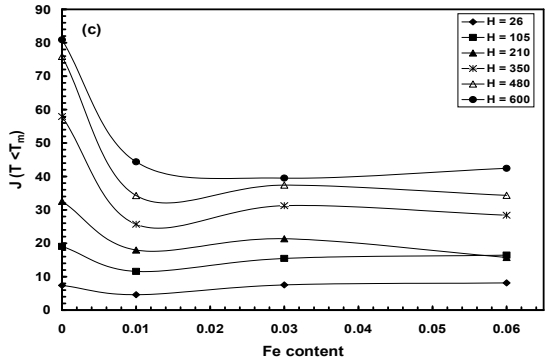

Figure 4(c): Critical current density J_c (T < Tm) against Fe content at different values of ac field amplitudes H_m

Table 1: Lattice parameters, orthorhombic distortion, onset of diamagnetism for pure and Fe doped $SmBa_2Cu_3O_7$ polycrystalline superconductor

Fe-content	a (Å)	b (Å)	c (Å)	OD	T_c (K)
0.00	3.816	3.886	11.683	0.018	90.3
0.01	3.819	3.881	11.684	0.016	90.0
0.03	3.836	3.867	11.683	0.008	88.5
0.06	3.854	3.854	11.681	0.000	83.3

Table (2): Values of a, q and αj(0) deduced from the fitting of the logarithmic plot relations, as a function of Fe-content

Fe-content	R(I)	$\alpha_j(0)$ [TA/m^2]	R(II)	$\alpha_j(0)$ [TA/m^2]
0.00	q = 0.56, aL = - 5.17	1177.85	q = 0.30, aL = - 3.79	1918.37
0.01	q = 0.34, aL = - 3.54	740.10	q = 0.87, aL = - 8.19	875.91
0.03	q = 0.66, aL = - 6.51	958.67	q = 0.83, aL = - 8.23	1880.87
0.06	q = 0.19, aL = - 3.65	1198.00	q = 0.91, aL = - 8.81	2163.27

Table (3): $J_c(T_m)$, χ' (T < T_m), Jc (T < T_m), χ' (T > T_m) and J_c (T > T_m) evaluated numerically as a function of AC field amplitude for pure sample.

H_m (A/m)	T_m (K)	J_c (T_m) A/cm^2	T < T_m (K)	χ' (T< T_m)	J_c (T<T_m) A/cm^2	T > T_m (K)	χ' (T > T_m)	J_c (T > T_m) A/cm^2
26	88.0	1.66	82.5	0.888	7.41	89.3	0.596	1.98
105	85.9	6.71	81.5	0.824	19.06	88.2	0.458	6.15
210	85.3	13.42	81.2	0.794	32.57	87.9	0.518	13.90
350	83.7	22.36	80.4	0.807	57.93	87.1	0.529	23.66
480	82.8	30.67	79.9	0.798	75.92	86.7	0.521	31.96
600	83.3	38.34	80.2	0.763	80.89	86.9	0.492	37.73

Table (4): $J_c(T_m)$, $\chi'(T < T_m)$, Jc $(T < T_m)$, χ' $(T > T_m)$ and J_c $(T > T_m)$ evaluated numerically as a function of AC field amplitude for Fe = 0.01 doped sample.

H_m (A/m)	T_m (K)	J_c (T_m) A/cm^2	$T < T_m$ (K)	χ' $(T< T_m)$	J_c $(T<T_m)$ A/cm^2	$T > T_m$ (K)	χ' $(T > T_m)$	J_c $(T > T_m)$ A/cm^2
26	87.7	0.98	82.4	0.894	4.62	88.9	0.234	0.46
105	86.8	3.96	81.9	0.829	11.58	88.4	0.333	2.64
210	86.5	7.92	81.8	0.780	18.00	88.3	0.345	5.46
350	86.0	13.2	81.5	0.743	25.68	88.0	0.379	10.00
480	84.9	18.11	80.3	0.736	34.30	87.5	0.450	16.30
600	83.6	22.64	79.5	0.745	44.39	86.8	0.459	20.78

Table (5): J_c (T_m), χ' $(T < T_m)$, Jc $(T < T_m)$, χ' $(T > T_m)$ and J_c $(T > T_m)$ evaluated numerically as a function of AC field amplitude for Fe = 0.03 doped sample.

H_m (A/m)	T_m (K)	J_c (T_m) A/cm^2	$T < T_m$ (K)	χ' $(T< T_m)$	J_c $(T<T_m)$ A/cm^2	$T > T_m$ (K)	χ' $(T > T_m)$	J_c $(T > T_m)$ A/cm^2
26	89.3	1.33	82.2	0.912	7.56	88.0	0.300	0.80
105	87.8	5.38	81.4	0.826	15.46	87.2	0.168	1.81
210	87.7	10.77	81.3	0.748	21.37	87.1	0.238	5.13
350	86.9	17.95	80.9	0.713	31.27	86.7	0.292	10.48
480	86.8	24.62	80.0	0.671	37.42	85.9	0.307	15.11
600	85.1	30.77	81.0	0.611	39.50	86.8	0.277	17.05

Table (6): $J_c(T_m)$, χ' $(T < T_m)$, Jc $(T < T_m)$, χ' $(T > T_m)$ and J_c $(T > T_m)$ evaluated numerically as a function of AC field amplitude for Fe = 0.06 doped sample.

H_m (A/m)	T_m (K)	J_c (T_m) A/cm^2	$T < T_m$ (K)	χ' $(T< T_m)$	J_c $(T<T_m)$ A/cm^2	$T > T_m$ (K)	χ' $(T > T_m)$	J_c $(T > T_m)$ A/cm^2
26	83.6	1.86	79.3	0.886	8.16	82.5	0.044	0.16
105	83.3	7.50	79.1	0.772	16.45	82.3	0.047	0.71
210	83.0	15.00	79.0	0.524	15.76	82.1	0.020	0.60
350	82.1	25.00	78.5	0.560	28.41	81.7	0.047	2.35
480	81.7	34.86	78.3	0.553	34.36	81.5	0.061	4.25
600	81.3	42.86	78.1	0.495	42.44	81.3	0.064	5.49

Conclusion

The effect of Fe doping on Flux pinning and critical current density of Sm: 123 superconducting system is investigated. Two different values of q obeying the law, $(1 - \frac{T_m}{T_c}) = a_L (H_m)^q$ are obtained for each sample. As compared to undoped sample, the pinning force density is decreased by 0.01 Fe additions, followed by an increase with further increase of Fe up to 0.06. Similar behavior could be obtained for critical current density. It is suggested that Fe doping up to a certain amount (0.06) improves the induced weak link profile, and consequently the pinning force density and critical current density are enhanced.

References

1. Bednorz J, Müller KA,, Z.Phys. B 1986, 64,1:189.
2. Chu C.W, Hor H, Meng R.L, Gao L, Huang K.J, Wang Y.Q, Phys. Rev. Lett. 1987, 58: 405.
3. Hettinger D, Swanson A.G, Skocpol W.J, Brooks J.S, Graybeal J.M, Mankiewich P.M, Howard R.E, stranghn B.L, Burkhardt E.G, Phys. Rev. Lett. 1989, 62: 2044.
4. Nikolo N and Goldfarb R.B, Phys. Rev. B 1988, 39: 6615.
5. Shinde S.L, Morrill J, Goland D, Chance D.A, McGuire T, Phys. Rev. B 1988, 41: 8838.

6. Mehbod M, Sergeenkov S, Ausloos M, Schroder J,. Dang A, Phys. Rev. B 1993, 48: 483.
7. Feng Y, Pradhan A.K, Zhao, Y Chen S.K, Wu Y, Zhang C.P, Yan G,Yau J.K.F, Zhou L, Koshizuka N, Physica C 2003, 385: 363.
8. Mahmoud A.S, Russell G.J, Koblischka M.R, Chikumoto N, Murakami M, Physica C 1998, 415: 40.
9. Müller K.H,, Physica C 1989, 159: 717.
10. Chen D.X, Nogues J, Rao K.V, Cryogenics 1989, 29: 800.
11. Sedky A, Youssif M.I J. Magn. Magn. Mater. 2001, 237: 22.
12. Gömöry F, Lobotka P, Solid State Commun. 1988, 66: 645.
13. Murphy S.D, Renouard K, Crittenden R, Bhagat S.M, Solid State Commun.1989, 69: 367.
14. Kumaraswamy B.V, Lal R, Narlikar A.V, Phys. Rev. B 1995, 53: 6759.
15. Ravi S, Bai V.S, Physica C 1994, 230: 51.
16. Ravi S, Physica C 1998, 295: 277.
17. Schilling O.F, Alhara A, Soeta A, Kamo T, Matsuda S, Phys. Rev. B 1993, 47: 8096.
18. Sedky A, Youssif M.I, Physica C 2004, 403: 297.
19. Mendoza E, Puig T, Varesi E, Carrillo A.E, Plain J, Obradors X, Physica C 2000, 334: 7.
20. Ilonca G, Yang T.R, Pop A.V, Stiufiuc G, Stiufiuc R, Lung C, Physica C 2003, 388-389: 425.
21. Lee J.H, Kim G.C, Kim Y.C, Jeong D.Y**,** Physica C 2005, 418: 131.
22. Nayak P.K, Ravi S, Solid State Commu. 2006, 138,8: 377.
23. Bean C.P, Rev. Mod. Phys. 1964, 36: 31.
24. Lan M.D, Liu J.Z, Shelton R.N, Phys. Rev. B 1991, 44: 2751.
25. Nikogosyan S.K, Sahakyan A.A, Yeritsyan H.N, Grigoryan V.A, Zargaryan E.G, Sarkissyan A.G, Physica C 1998, 299: 65.
26. Gupta A, Lal R, Sedky A, Narlikar A.V, Awana V.P.S, Phys. Rev. B 2001, 61: 11752.
27. Wordenweber R, Heinemann K, Sastry G.V.S, Freyhardt H.C, Physica C 1989, 162 -164: 1601.
28. Asaturian R.A, Sarkissian A.G, Ignatian E.L, Begoian K.G**,** Solid State Commun. 1995, 95: 389.
29. Ruppel S, Michels G, Geus H, Schlabitz W, Roden B, Wohlleben D, Physica C 1991, 174: 233.
30. Sedky A, Youssif M.I, Khalil S.M, Ayman Sawala, Solid State Commun. 2006, 139: 126.
31. Celebi S, Kölemen U, Malik A.L Öztürk A, Phys. Stat. Sol. (a) 2001, 194: 260.

5/19/2015